Adsorption Capacity of Mesoporous SBA-15 Particles Synthesized from Corncobs and Rice Husk at Different CTAB/P123 Ratios and Their Application for Dyes Adsorbent

Dhaneswara, Donanta
Department of Metallurgy and Materials Engineering Universitas Indonesia, Kampus UI Depok

Zulfikar, Najla
Department of Metallurgy and Materials Engineering Universitas Indonesia, Kampus UI Depok

Jaka Fajar Fatriansyah
Department of Metallurgy and Materials Engineering Universitas Indonesia, Kampus UI Depok

Mohd Sufri Mastuli
School of Chemistry and Environment, Faculty of Applied Sciences, Universiti Teknologi MARA

他

https://doi.org/10.5109/6792887

出版情報：Evergreen. 10 (2), pp.924-930, 2023-06. 九州大学グリーンテクノロジー研究教育センター
バージョン：

Adsorption Capacity of Mesoporous SBA-15 Particles Synthesized from Corncobs and Rice Husk at Different CTAB/P123 Ratios and Their Application for Dyes Adsorbent

Donanta Dhaneswara[1,*], Najla Zulfikar[1], Jaka Fajar Fatriansyah[1], Mohd Sufri Mastuli[2,3], Iping Suhariadi[4]

[1]Department of Metallurgy and Materials Engineering Universitas Indonesia, Kampus UI Depok, 16424, Indonesia

[2]School of Chemistry and Environment, Faculty of Applied Sciences, Universiti Teknologi MARA, 40450 Shah Alam, Selangor, Malaysia

[3]Centre for Functional Materials and Nanotechnology, Institute of Science, Universiti Teknologi MARA, 40450 Shah Alam, Selangor, Malaysia

[4]Department of Industrial Engineering, Faculty of Engineering, Bina Nusantara University, Jakarta, 11480, Indonesia

*Author to whom correspondence should be addressed:
E-mail: donanta.dhaneswara@ui.ac.id

(Received January 20, 2023; Revised March 7, 2023; accepted April 17, 2023).

Abstract: Mesoporous silica can be a dye adsorbent to overcome related environmental problems. In this report, the extraction of mesoporous SBA-15 from corncob ash (CCA) and rick husk ash (RHA) at different mass ratios between cetyltrimethyl ammonium bromide (CTAB) and pluronic (P123) were investigated. The crystalline structure, chemical composition, morphology, and surface area of the silica were characterized by small-angle X-ray scattering (SAXS), Fourier-transform infrared spectroscopy (FTIR), scanning electron microscopy (SEM), and Brunauer–Emmett–Teller (BET). Experimental results indicated that the mesoporous SBA-15 from both CCA and RHA could be obtained with P123/CTAB ratios of 3:1 and 1:1. The findings of this study showed that mesoporous silica produced from corn cobs with a surfactant mass ratio of 1:1 had the highest surface area and adsorption capacity. The resulting silica mesopore had a pore diameter of 6.24 nm and a surface area of 425.12 m2/g. As a result, the mesoporous silica effectively adsorbed methylene blue dye and partially adsorbed methylene orange dye with an adsorption capacity of 2.6 mg/g after 3 hours of the adsorption process. The highest adsorption capacity for mesoporous silica made from rice husk was 2.26 mg/g. This study proves that the mesoporous silica formed has a certain degree of selectivity and adsorbs cationic dyes better than anionic ones, indicating its potential for liquid chromatography applications.

Keywords: Sustainability; Mesoporous silica; Adsorbent; Dye; Wastewater treatment

1. Introduction

Indonesia has an alarming water contamination issue that concerns researchers today. [1)] The textile industry is one of those industries that spills wastewater into the water system. Most of the textile industry uses synthetic dyes. These dyes are proven to be harmful to aquatic life and reported to be highly toxic and carcinogenic in nature.[2)] To fulfill the need for clean water, the government requires industries to have a wastewater treatment before disposing the water into the river.

The wastewater plant ideally consists of five stages.[3)] Among those stages, the fourth stage, which is filtration, is the most crucial stage that can be performed through the adsorption method utilizing an adsorbent.[4)] For large-scale industrial applications, the adsorbent must have a high absorption capacity and a reasonably low cost. One of the suitable materials to be used as adsorbents is mesoporous silica.[5)] To date, tetraalkoxysilanes are the most widely used starting materials for mesoporous silica owing to their high purity of silica content. Various mesoporous silica structures such as SBA-15, SBA-16, and MCM-41 can be produced by using this precursor containing tetraalkoxysilanes.[6,7,8)] Nonetheless, tetraalkoxysilanes is relatively expensive therefore it is not economically

favorable.[9]

Based on previous studies, agricultural wastes such as corn cob ash (CCA) and rice husk ash (RHA) have been successfully utilized as silica sources for mesoporous silica.[10,11] However, producing well-ordered mesoporous silica from natural sources with performance on par with tetraalkoxysilanes derived mesoporous silica is still very challenging due to the differences in the purity of silica precursors where the silica from natural sources generally still contain some small impurities.[12] One of strategies to improve the microstructure of mesoporous silica is by introducing surfactants and co-surfactants.[13] While a well-structured mesoporous silica with unique particle shape can be obtained by controlling surfactant content,[14] nonetheless to our knowledge there is no study on the effect of co-surfactant on the mesoporous silica synthesized from RHA and CCA. In this study, a co-surfactant was added to engineer the shape and characteristics of the pores that would be formed. In addition, we will demonstrate the performance of mesoporous silica in adsorbing a mixture of methylene blue and methylene orange dyes which represent anionic and cationic dyes in textile waste.

2. Experimental

Corn cobs and rice husks were washed and dried under the sun for 6 hours, followed by separate combustion at 700˚C for 6 hours. The resulted corn cob ash (CCA) and rice husk ash (RHA) were weighed for 5 g and dissolved in 100 ml of 10% w/v NaOH solution, then the mixture was incubated for 24 hours and refluxed at 80˚C for 1 hour. This refluxed solution was then filtered to obtain a solution of sodium silica as a silica precursor. The mixture of P123 and CTAB were used as surfactant with ratio of 1:0, 3:1, 1:1, and 1:3 ratio which were referred to V1, V2, V3, and V4, respectively. Each variation was then dissolved in 380 mL of 1.6 M HCl. Then, every 380 mL of the surfactant solution was reacted with 200 mL of sodium silica precursor and was heated at 40˚C for 24 hours to form gel. The formed gel was dried at 100˚C for 24 hours. The formed precipitate was dried at 100˚C for 8 hours. The dried substrate was then calcined at 500˚C for 6 hours with a heating rate of 10˚C per minute and cooled to room temperature.

The crystalline structure of the samples was characterized by small-angle X-ray scattering (SAXS) using Shimadzu XD-610. The surface morphology of the mesoporous silica was investigated by scanning electron microscopy (SEM) using FEI Inspect F50 machine. The chemical composition and functional group of the mesoporous silica were characterized by Fourier-transform infrared spectroscopy (FTIR) using Perkin Elmer UATR two machines. The surface area of the mesoporous silica was studied by Brunauer–Emmett–Teller (BET) using Quantachrome Instrument NOVA Station A. The dye solution for the adsorption test was prepared by dissolving 8 mg of Methylene Blue (MB) and Methylene Orange (MO) powders in 800 mL of distilled water. 50 mg of mesoporous silica was added to a 50 ml dye solution. The solution was placed in a magnetic stirrer for 3 hours at a speed of 200 rpm. Every 1 hour, 7 mL of the solution was taken and characterized by UV-VIS using Perkin Elmer UV-Vis Spectrophotometer Lambda 25. The dye removal efficiency (%R) and adsorbate uptake (q) were calculated using the equation (1) and (2) taken from the previous research:[15]

$$q = \frac{(C_0 - C)\, x\, V}{m} \qquad (1)$$

$$\%R = \frac{C_0 - C}{C_0} \text{ x } 100\% \qquad (2)$$

3. Results and Discussion

Fig. 1 shows the SAXS graphs for RHA and CCA synthesized at various P123/CTAB ratios. For both CCA and RHA, only sample V2 and V3 exhibit mesoporous structure associated by the presence of three peaks which are belong to 2D hexagonal (*p6mm*) symmetry of SBA-15.[16,17] The CCA and RHA samples have the same trend for the order of samples with the highest to lowest peak intensities, that is, V2 > V3 > V4 >V1.

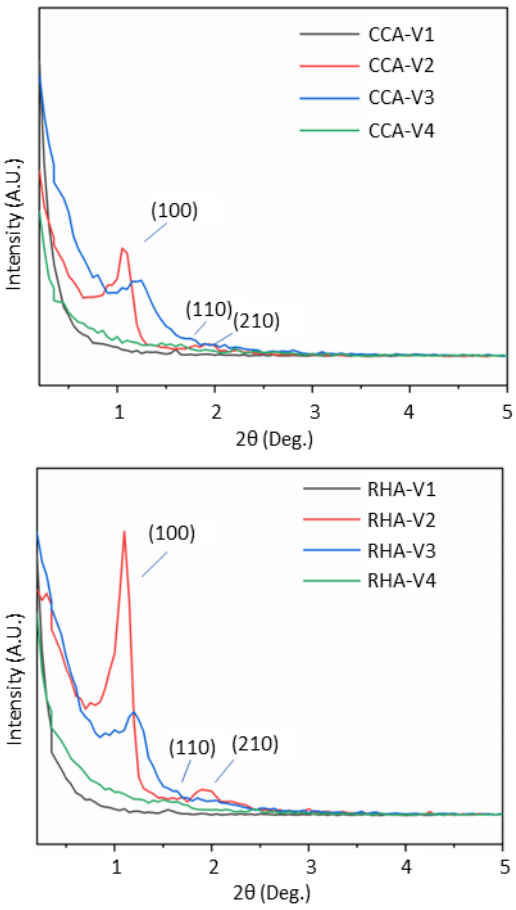

Fig. 1. SAXS graph of CCA and RHA samples.

This result proves that the added CTAB increased the pores' regularity in the samples. The CTAB, as a cationic surfactant, formed micelles with positively charged headgroups. Consequently, the shape of the micelles is more regular as the charges separate them at a certain distance uniformly. [18] However, there is a maximum dose of CTAB that can be added as a co-surfactant to P123 in order to maximize the regularity of the micelles.[19] Insufficient P123, as a non-cationic surfactant, also causes poor pores regularity and low structure stability.

Fig. 2 shows the FTIR spectra of CCA and RHA samples obtained at four P123 and CTAB surfactant ratios. It is visible that there is a transmission peak at wave numbers between 440 – 470 cm^{-1}, 801 – 795 cm^{-1}, and at 1059 – 1073 cm^{-1}, which suggests the presence of Si-O-Si type of bonds.[20] Mesopore silica from CCA and RHA samples also has a weak peak at wave numbers 3402-3418cm^{-1} and 3392-3403cm^{-1}. These wave numbers indicate that both mesopore silicas have symmetrical and asymmetrical O-H stretching vibration groups. The existence of this group comes from the presence of absorbed water molecules and the presence of the Si-OH group.[21] Other functional groups related to the structure of water were also found in the wave number range of 1640-1643cm^{-1}, which indicated the presence of H-O-H groups on both mesopore silicas from CCA and RHA.[22]

Fig. 3 shows the SEM micrograph of the prepared samples. As can be seen, spherical particles grow as CTAB increases, but aggregated particles considerably decrease.

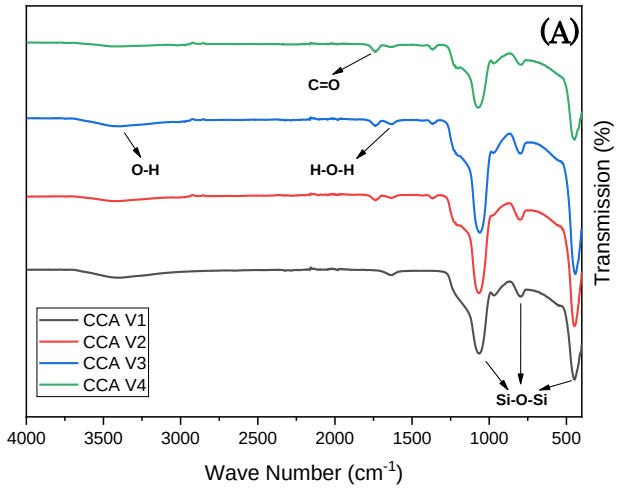

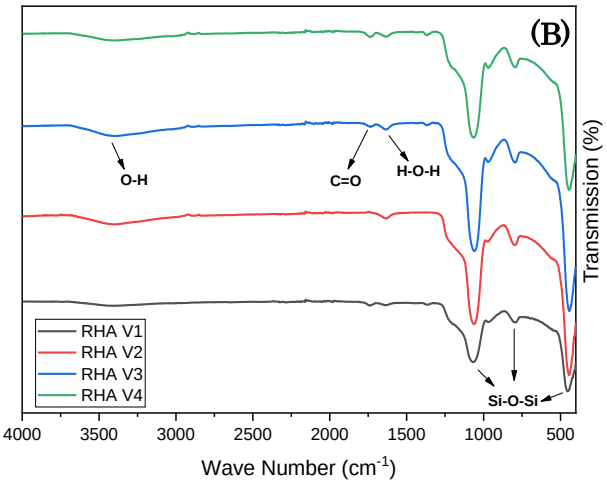

Fig. 2 Comparison of FTIR spectra of (A) CCA and (B) RHA mesoporous silica samples.

In CCA V3 and RHA V3, almost all particles are well dispersed. This dispersion is due to the morphology of the micelles being significantly affected by the packing parameters of the surfactant, namely the ah/ac ratio, where ah is the effective headgroup area and ac is the length of the hydrophobic chain. The greater the value of ah/ac, the more micelles tend to have a spherical morphology.[23] Therefore, the CTAB will react with the PPO tail and increase the ah/ac ratio. The addition of CTAB also reduces the tendency of particle aggregation due to electrostatic repulsive forces.[24,25] However, further addition of CTAB, represented by CCA V4 and RHA V4, caused the spherical particles to form an agglomerate. This agglomeration occurs because, when the concentration of CTAB is too high, the hydrophobic bonds will be present in the solution [26].

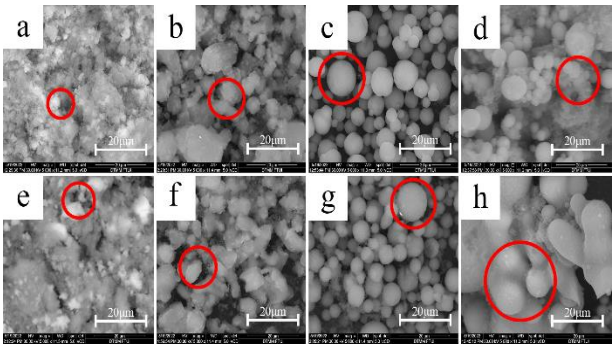

Fig. 3 SEM micrograph of the prepared mesoporous silica as the concentration ratio of P123 and CTAB increased: (a) RHA V1; (b) RHA V2; (c) RHA V3; (d) RHA V4; (e) CCA V1; (f) CCA V2; (g) CCA V3; and (h) CCA V4.

Fig. 4 shows the adsorption-desorption isotherms of all the CCA and RHA samples. It can be seen that the four samples have a type IV physisorption isotherm, which means that the four samples have a mesoporous shape.[27] According to IUPAC, the CCA V1 and RHA V1 have the shape of an H3 loop hysteresis curve, while the CCA V2 and V3 formed hysteresis loops H2 (b) and H2 (a) shape, and CCA V4 had an H4 loop hysteresis curve.[28]

Comparations of the pore diameters and the surface area of the samples are shown in Fig. 5. The CCA and RHA formed a similar trend, where V2 has the largest diameter, 6.25 nm and 6.18 nm, followed by V3, V4, and V1. According to the literature, adding co-surfactant CTAB to P123 reduces the pore size.[29] However, in V1, there is a discrepancy with the literature. This phenomenon is due to the unstable temperature during the ageing process. The difference in pore shape and diameter significantly influences the surface area formed. It can be seen that the samples with the largest surface area are CCA and RHA V3, with values of 425.12 m^2/g and 389.26 m^2/g then, followed by V2, then V1, and V4.

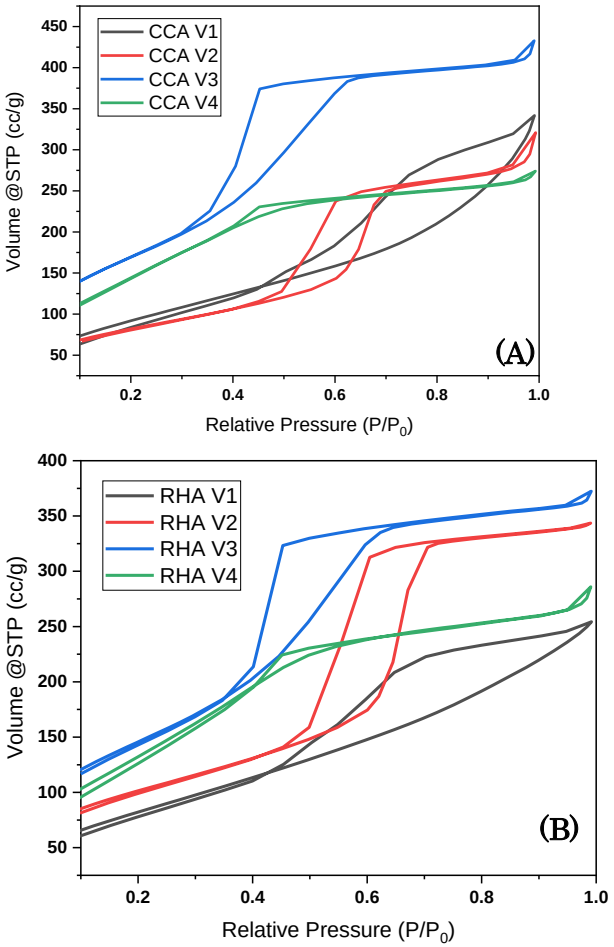

Fig. 4 Adsorption-desorption isotherms of mesoporous silica of (A) CCA and (B) RHA samples.

In Fig. 6, the colour of the synthetic dye solution changes with increasing absorption time by the mesoporous silica material. The UV-VIS spectrum of the blank solution can be seen in Fig. 7(A). A peak at a wavelength of around 675 cm^{-1} indicates the MB, [30] and at 463 cm^{-1}, indicating MO's presence.[31] Fig. 7(B) shows a UV-Visible graph of CCA after the adsorption process for 3 hours. The CCA and RHA samples of other variables showed the same trend. The graph does not show any peaks on the longer wavelength side that correlate to the presence of MB after the adsorption process occurs. This proves that all samples can absorb MB dye directly. This absorption is because mesoporous silica is negatively charged at neutral pH and adsorbs cationic MB through an electrostatic interaction mechanism.[32,33] A peak at a wavelength between 463 – 464 cm^{-1} means mesoporous silica has lower effectiveness in the absorption of MO dyes. Since MO is an anionic dye, there will be a repulsive interaction between MO and the silica so that silica can only interact through weak Van Der Waals forces or hydrogen bonds.[29]

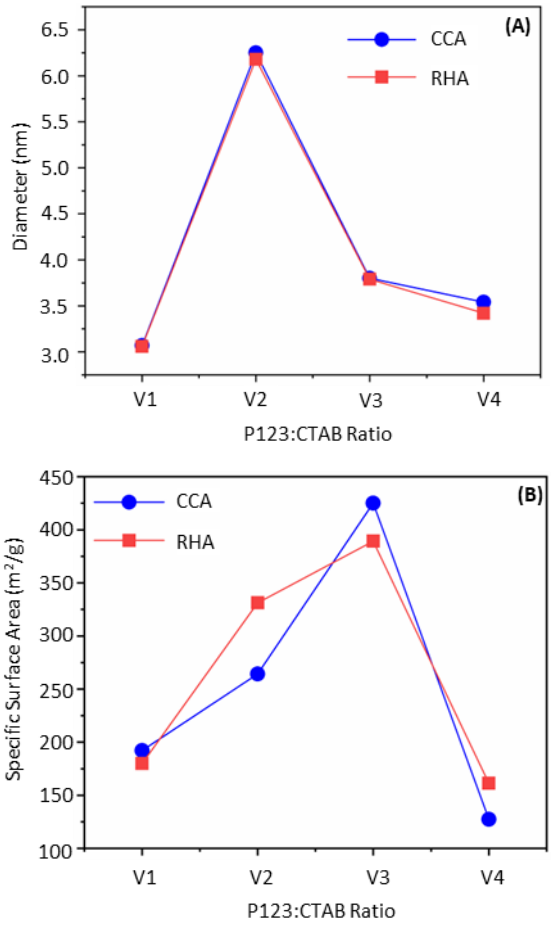

Fig. 5 Comparison of CCA and RHA (A) pore diameter and (B) surface area.

Fig. 8 compares the dye's absorbance capacity for each variable. The graph shows that CCA V3 and RHA V3 have the highest adsorption capacities of MO dyes after 3 hours of absorption compared to other samples, which is 2.6 mg/g and 2.26 mg/g, respectively. The adsorption capacity of CCA is higher than RHA due to the higher CCA surface area. The adsorption capacity is linearly related to the surface area since a higher surface area means more sites where MO substances can interact with silica. The graph also proves that both CCA and RHA samples are somewhat selective. The sample is only selective to a certain degree and can absorb MO anionic dyes in small amounts.

Fig. 6 Adsorption of the mixture of methylene blue and methylene orange by mesoporous silica (CCA-V3) during (a) 0 hours, (b) 1 hour, (c) 2 hours, and (d) 3 hours.

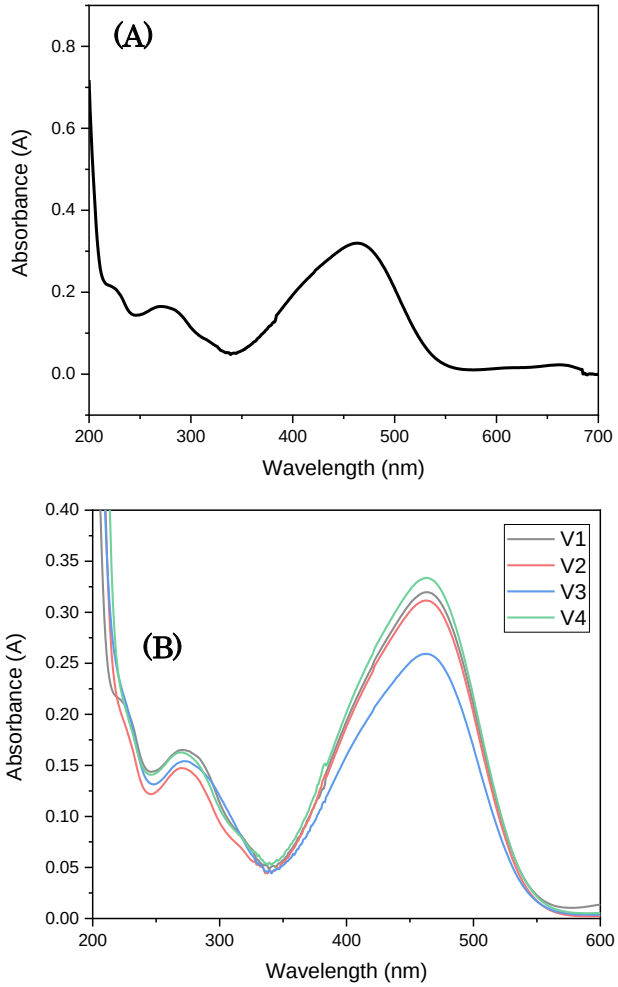

Fig. 7 UV-VIS spectra of (A) blank solution and (B) solution after 3 hours of adsorption process by CCA samples.

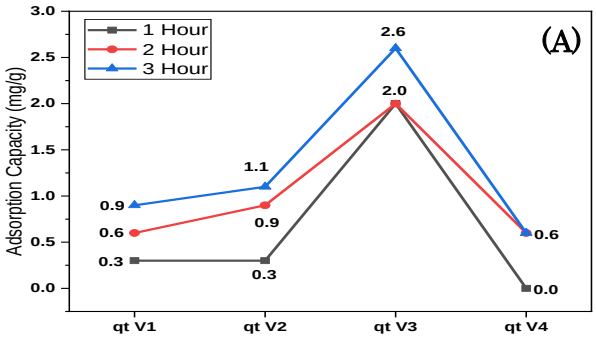

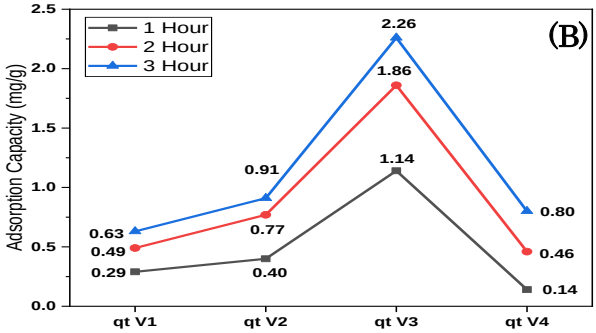

Fig. 8 Adsorption capacity of (A) CCA and (B) RHA silica mesoporous materials.

4. Conclusion

The concentration of CTAB added as a co-surfactant affects the characteristics of the pores. Increasing the CTAB/P123 surfactant ratio is found to form mesoporous silica with a higher surface area. Based on the UV-VIS results, mesoporous silica's ability to adsorb cationic dyes (MB: Methylene Blue) is more effective than its ability to absorb anionic dye (MO: Methyl Orange). The UV-VIS results also found that increased CTAB/P123 surfactant ratios would cause more MO dye to be adsorbed. The adsorption ability of methylene dye on mesoporous silica is directly proportional to its surface area. Therefore, CCA and RHA samples selectively absorb cationic dyes and can also absorb anionic dyes to a certain degree indicating its potential for liquid chromatography.

Acknowledgements

The work was supported by a research grant from the Internationally Indexed Publication Grant (PUTI) Q2 Batch 2, NKB-1328/UN2.RST/HKP.05.00/2022.

Nomenclature

q	uptake capacity at time t (mg. g^{-1})
C_0	initial concentration (mg. L^{-1})
C	concentration at time t (mg. L^{-1})
m	mass of adsorbent (g)
V	volume (L)
%R	removal (%)

Abbreviation table

SBA-15/16	Santa Barbara Amorphous-15/16
CTAB	Cetyl trimethylammonium bromide
P123	Pluronic 123
SAXS	small-angle X-ray scattering
FTIR	Fourier-transform infrared spectroscopy
SEM	scanning electron microscopy
CCA	corncobs ash
RHA	rick husk ash
MCM-41	Mobil Composition of Matter-41
MB	Methylene Blue

MO Methylene Orange
UV-VIS Ultraviolet–visible

References

1) Y. Iriani, R. Afriani, D.K. Sandi, and F. Nurosyid, "Co-precipitation synthesis and photocatalytic activity of mn- doped srtio 3 for the degradation of methylene blue wastewater," *Evergreen*, **09** (*04*) 1039–1045 (2022). doi.org/10.5109/6625717
2) R. Krishnamoorthy, A.R. Choudhury, P.A. Jose, K. Suganya, M. Senthilkumar, J. Prabhakaran, N.O. Gopal, J. Choi, K. Kim, R. Anandham, and T. Sa, "Long-term exposure to azo dyes from textile wastewater causes the abundance of saccharibacteria population," *Appl. Sci.*, **11** (*1*) 1–8 (2021). doi:10.3390/app11010379.
3) G.Z. Kyzas, and K.A. Matis, "Wastewater treatment processes: part i," *Processes*, **8** (*3*) (2020). doi:10.3390/pr8030334.
4) A.H. Jawad, S.H. Mallah, and M.S. Mastuli, "Adsorption behavior of methylene blue on acid-treated rubber (hevea brasiliensis) leaf," *Desalin. Water Treat.*, **124** (*November*) 297–307 (2018). doi:10.5004/dwt.2018.22915.
5) S. Kim, Y. Han, J. Park, and J. Park, "Adsorption characteristics of mesoporous silica sba-15 synthesized from mine tailing," *Int. J. Miner. Process.*, **140** 88–94 (2015). doi:10.1016/j.minpro.2015.04.027.
6) M. Naghiloo, M. Yousefpour, M.S. Nourbakhsh, Z. Taherian, Functionalization of SBA-16 silica particles for ibuprofen delivery, Journal of Sol-Gel Science and Technology, 74 (2015) 537-543.
7) S. Kingchok, S. Pornsuwan, Comparison of spherical and rod-like morphologies of SBA-15 for enzyme immobilization, *J. Porous Mater.*, **27** (2020) 1547-1557.
8) C.C. Pantazis, P.N. Trikalitis, P.J. Pomonis, M.J. Hudson, A method of synthesis of silicious inorganic ordered materials (MCM-41–SBA-1) employing polyacrylic acid–CnTAB–TEOS nanoassemblies, *Microporous Mesoporous Mater.*, **66** (2003) 37-51.
9) S. Silviana, A.G. Hasega, A. Rizqy, N. Hanifah, and A. Ni, "Synthesis of silica coating derived from geothermal solid waste modified with 3-aminopropyl triethoxysilane (aptes) and silver nano particles (agnps)," *Evergreen*, **09** (*04*) 1224–1230 (2022). doi.org/10.5109/6625733
10) H. Al Hijri, J.F. Fatriansyah, N. Sofyan, and D. Dhaneswara, "Potential use of corn cob waste as the base material of silica thin films for anti-reflective coatings," *Evergreen*, **9** (*1*) 102–108 (2022). doi:10.5109/4774221.
11) D. Dhaneswara, J.F. Fatriansyah, F.W. Situmorang, and A.N. Haqoh, "Synthesis of amorphous silica from rice husk ash: comparing hcl and ch3cooh acidification methods and various alkaline concentrations," *Int. J. Technol.*, **11** (*1*) (2020). doi:10.14716/ijtech.v11i1.3335.
12) S. Pimprom, K. Sriboonkham, P. Dittanet, K. Föttinger, G. Rupprechter, P. Kongkachuichay, Synthesis of copper–nickel/SBA-15 from rice husk ash catalyst for dimethyl carbonate production from methanol and carbon dioxide, *J. Ind. Eng. Chem.*, **31** (2015) 156-166.
13) D. Gao, A. Duan, X. Zhang, K. Chi, Z. Zhao, J. Li, Y. Qin, X. Wang, C. Xu, Self-assembly of monodispersed hierarchically porous Beta-SBA-15 with different morphologies and its hydro-upgrading performances for FCC gasoline, *J. Mater. Chem. A*, **3** (2015) 16501-16512.
14) D. Dhaneswara, H.S. Marito, J.F. Fatriansyah, N. Sofyan, D.R. Adhika, and I. Suhariadi, "Spherical sba-16 particles synthesized from rice husk ash and corn cob ash for efficient organic dye adsorbent," *J. Clean. Prod.*, **357** (*July*) 1–9 (2022). doi:10.1016/j.jclepro.2022.131974.
15) A. Azani, D.S.C. Halin, M.M. Al Bakri Abdullah, K.A. Razak, M.F.S.A. Razak, M.M. din Ramli, M.A.A.M. Salleh, and V. Chobpattana, "The effect of go/tio2 thin film during photodegradation of methylene blue dye," *Evergreen*, **8** (*3*) 556–564 (2021). doi:10.5109/4491643.
16) E.M. Björk, "Mesoporous Building Blocks: Synthesis and Characterization of Mesoporous Silica Particles and Films," Linköping University, 2013. doi:10.3384/diss.diva-99858.
17) D. Zhao, J. Feng, Q. Huo, N. Melosh, G.H. Fredrickson, B.F. Chmelka, and G.D. Stucky, "Triblock copolymer syntheses of mesoporous silica with periodic 50 to 300 angstrom pores," *Science (80-.).*, **279** (*5350*) 548–552 (1998). doi:10.1126/science.279.5350.548.
18) C. Gao, H. Qiu, W. Zeng, Y. Sakamoto, O. Terasaki, K. Sakamoto, Q. Chen, and S. Che, "Formation mechanism of anionic surfactant-templated mesoporous silica," *Chem. Mater.*, **18** (*16*) 3904–3914 (2006). doi:10.1021/cm061107+.
19) H. Iván Meléndez-Ortiz, B. Puente-Urbina, G. Castruita-De Leon, J.M. Mata-Padilla, and L. García-Uriostegui, "Synthesis of spherical sba-15 mesoporous silica. influence of reaction conditions on the structural order and stability," *Ceram. Int.*, **42** (*6*) 7564–7570 (2016). doi:10.1016/j.ceramint.2016.01.163.
20) N. Rameli, K. Jumbri, R.A. Wahab, A. Ramli, and F. Huyop, "Synthesis and Characterization of Mesoporous Silica Nanoparticles Using Ionic Liquids As A Template," in: IOP Conf. Ser. J. Phys., 2018. doi:10.1088/1742-6596/1123/1/012068.
21) M. Rubaya Rashid, F. Afroze, S. Ahmed, M.S. Miran, and M. Abu Bin Hasan Susan, "Control of The Porosity and Morphology of Ordered Mesoporous Silica by Varying Calcination Conditions," in: Mater. Today Proc., Elsevier Ltd., 2019: pp. 546–554. doi:10.

1016/j.matpr.2019.04.119.
22) B. Baumgartner, J. Hayden, J. Loizillon, S. Steinbacher, D. Grosso, and B. Lendl, "Pore size-dependent structure of confined water in mesoporous silica films from water adsorption/desorption using atr-ftir spectroscopy," *Langmuir*, **35** (*37*) 11986–11994 (2019). doi:10.1021/acs.langmuir.9b01435.
23) Z. Lin, J.J. Cai, L.E. Scriven, and H.T. Davis, "Spherical-to-wormlike micelle transition in ctab solutions," *J. Phys. Chem.*, **98** (*23*) 5984–5993 (1994). doi:10.1021/j100074a027.
19) H. Vatanparast, F. Shahabi, A. Bahramian, A. Javadi, and R. Miller, "The role of electrostatic repulsion on increasing surface activity of anionic surfactants in the presence of hydrophilic silica nanoparticles," *Sci. Rep.*, **8** (*1*) (2018). doi:10.1038/s41598-018-25493-7.
24) Salwa M.I. Morsy, "Role of surfactants in nanotechnology and their applications," *Int.J.Curr. Microbiol.App.Sci*, **3** (*5*) 237–260 (2014).
25) Y. Liu, M. Tourbin, S. Lachaize, and P. Guiraud, "Silica nanoparticles separation from water: aggregation by cetyltrimethylammonium bromide (ctab)," *Chemosphere*, **92** (*6*) 681–687 (2013). doi:10.1016/j.chemosphere.2013.03.048.
26) K.S.W. Sing, D.H. Everett, R.A.W. Haul, L. Moscou, R.A. Pierotti, J. Rouquerol, and T. Siemieniewska, "Reporting physisorption data for gas/solid systems with special reference to the determination of surface area and porosity," *Pure Appl. Chem.*, **57** (*4*) 603–619 (1985). doi:10.1351/pac198557040603.
27) L. Xu, J. Zhang, J. Ding, T. Liu, G. Shi, X. Li, W. Dang, Y. Cheng, and R. Guo, "Pore structure and fractal characteristics of different shale lithofacies in the dalong formation in the western area of the lower yangtze platform," *Minerals*, **10** (*1*) 1–25 (2020). doi:10.3390/min10010072.
28) E.M. Johansson, "Controlling the Pore Size and Morphology of Mesoporous Silica," LiU-tryck, 2010.
29) W.R. Algar, C.A.G. De Jong, E.J. Maxwell, and C.G. Atkins, "Demonstration of the spectrophotometric complementary color wheel using leds and indicator dyes," *J. Chem. Educ.*, **93** (*1*) 162–165 (2016). doi:10.1021/acs.jchemed.5b00665.
30) S.I. Orozco, L.M. Blanco, M.A. Garza, V.A. González, C. Borrás, and B. Sharifker, "Phenol degradation using glassy carbon electrodes modified with particles of co-mo alloy," *Int. J. Electrochem. Sci.*, **8** (*4*) 5698–5709 (2013).
31) B. Boukoussa, A. Hakiki, S. Moulai, K. Chikh, D.E. Kherroub, L. Bouhadjar, D. Guedal, K. Messaoudi, F. Mokhtar, and R. Hamacha, "Adsorption behaviors of cationic and anionic dyes from aqueous solution on nanocomposite polypyrrole/sba-15," *J. Mater. Sci.*, **53** (*10*) 7372–7386 (2018). doi:10.1007/s10853-018-2060-7.
32) N. Yuan, H. Cai, T. Liu, Q. Huang, and X. Zhang, "Adsorptive removal of methylene blue from aqueous solution using coal fly ash-derived mesoporous silica material," *Adsorpt. Sci. Technol.*, **37** (*3–4*) 333–348 (2019). doi:10.1177/0263617419827438.
33) S.O. Akpotu, and B. Moodley, "Effect of synthesis conditions on the morphology of mesoporous silica from elephant grass and its application in the adsorption of cationic and anionic dyes," *J. Environ. Chem. Eng.*, **6** (*4*) 5341–5350 (2018). doi:10.1016/j.jece.2018.08.027.